Journal of Alloys and Compounds 576 (2013) 363–368

Contents lists available at SciVerse ScienceDirect

Journal of Alloys and Compounds

journal homepage: www.elsevier.com/locate/jalcom

Study of the focusing effect of silica microspheres on the upconversion of Er^{3+}–Yb^{3+} codoped glass ceramics

C. Pérez-Rodríguez [a,*], M.H. Imanieh [b,c], L.L Martín [a], S. Ríos [d], I.R. Martín [a,e], Bijan Eftekhari Yekta [c]

[a] Dpto. Física Fundamental y Experimental, Electrónica y Sistemas, Universidad de La Laguna, Av. Astrofísico Francisco Sánchez, s/n E-38206 La Laguna, Tenerife, Spain
[b] Department of Chemical and Environmental Engineering, University of Toledo, Toledo, OH, USA
[c] Department of Materials, Ceramic Division, Iran University of Science and Technology, Tehran, Iran
[d] Dpto. de Física Básica, Universidad de La Laguna, Av. Astrofísico Francisco Sánchez, s/n E-38206 La Laguna, Tenerife, Spain
[e] MALTA Consolider Team, Av. Astrofísico Francisco Sánchez, s/n E-38206 La Laguna, Tenerife, Spain

ARTICLE INFO

Article history:
Received 22 February 2013
Received in revised form 8 May 2013
Accepted 31 May 2013
Available online 10 June 2013

Keywords:
Optical properties
Optical spectroscopy
Luminescence
Rare Earth alloys and compounds
Optical material

ABSTRACT

The upconversion emission properties of Er^{3+}–Yb^{3+} codoped glass and glass ceramic samples with different Si/Al ratios and thermal treatments were analyzed by covering their surfaces with silica microspheres (3.8 μm diameter). A 950 nm laser beam is focused by the microspheres producing a set of photonic nanojets near the surface of the samples. After the upconversion processes of the Er^{3+} ions located in each microsphere focus area, these ions emit light in the green and red regions. The red emission from each sample was measured, yielding an upconversion intensity in the focal areas three times higher than the emission from the bare substrate. To estimate the real size of the red emission area under a single microsphere, a deconvolution of the measured focal spots with the Point Spread Function of the experimental setup was performed, resulting in a Full Width at Half Maximum of 330 nm. The results obtained by Finite-Difference Time-Domain simulations are in good agreement with the experimental values.

1. Introduction

The employment of nanoscale materials as sensors seems advantageous since they confer local resolution while avoiding the spread of damaging perturbations in those systems in which they are used. These materials are of special interest in the field of biology, where they can be used simultaneously as nanothermometers and to produce a localized thermal treatment in a biological sample [1]. Research on new label probes [2] is also interesting in other fields, like microscopy. Efficient emitters are a key to achieving these goals, with non-toxicity being an additional requirement for biological applications. This explains the current trend of conducting research on obtaining sufficiently high optical intensities in nanoemitters [3,4]. However, this requirement on emitter efficiency when the sources have a reduced size is not a trivial issue [5], despite the emergence of low signal detectors that simplify the measurements of emissions from discretely incorporated nanoparticles.

Upconversion processes (UC) among Rare Earth (RE) ions are characterized by the sequential absorption of two or more photons that lead to the emission of light at wavelengths below the excitation wavelength. Upconversion emitters are starting to be considered as advantageous probes for fluorescence microscopy imaging because their luminescence is stable over time, their variety covers a wide spectral range and they can be synthesized as nanoparticles [6]. In an effort to improve the efficiency of the RE upconversion luminescence, different strategies are used, such as the design of the glass compositions, the combinations of different RE ions and the variation of doping concentrations, as well as the application of thermal treatments. With regard to this last approach, it was discovered that in many glass samples nanocrystals may appear after the thermal treatment, allowing the RE to be incorporated into these nanocrystals, thus improving their luminescence. Materials that combine a glass amorphous matrix with immersed nanocrystallites are known as glass ceramics. In general, the upconversion efficiency is higher with optimized glass ceramics as compared to the precursor glass since the distances between the RE ions in the crystallites of the former are shortened, favoring energy transfer among the ions. Additionally the crystalline phase in which the RE emitters are immersed results in decreased optical losses due to the reduction of the higher energy phonons [7,8].

Microspheres have been used to produce focal regions, known as photonic nanojets [9,10], whose sizes are below the micrometric scale. Previous research [11–14] has demonstrated experimentally and with simulations the use of microspheres in order to increase the signal intensity obtained in different experiments. In Ref. [11],

* Corresponding author. Tel.: +34 922318651.
E-mail address: cjperez@ull.edu.es (C. Pérez-Rodríguez).

0925-8388/$ - see front matter © 2013 Elsevier B.V. All rights reserved.
http://dx.doi.org/10.1016/j.jallcom.2013.05.222

the authors reported a confirmation of the photonic jet in the microwave scale, observing the backscattering enhancement that occurred when metallic particles where introduced in the focus area. This backscattered emission was also analyzed in Refs. [12,13] but using dielectric microspheres illuminated in the optical range. In Ref. [12] a measurable enhancement of the backscattered light in the visible range was obtained when a gold nanoparticle was placed inside the photonic nanojet region produced by a dielectric microsphere with a 4.4 μm diameter. The authors concluded that this property could be advantageous for the visible detection of metallic nanoparticles even with diameters below 50 nm. In the work in Ref. [13], Hill et al. reported the backward emission from the fluorescence of a dye droplet excited with one, two or three photons. Moreover, Lecler et al. [14] measured a 30% increase in the fluorescence of a rhodamine B solution doped with microspheres. However, to our knowledge the use of nanojets produced by transparent microspheres in order to excite optical active materials, under upconversion processes with different numbers of excitation photons, has not been analyzed in the literature.

The aim of this work is to magnify the signal sent out by a small UC emitter by means of silica microspheres. These microspheres act as lenses focusing the excitation on the emitter and also collecting its luminescence towards the detector. Er^{3+}–Yb^{3+} ions were included as codoping ions in the composition of glass and glass ceramic samples of a biologically compatible matrix, and their red upconversion emission was studied. This matrix corresponds to an oxyfluoride glass in which CaF_2 nanocrystals are formed under different thermal treatments. In these samples an efficient energy conversion of the 950 nm excitation wavelength occurs by the action of the Er^{3+}–Yb^{3+} ions, resulting in an intense 650 nm emission.

In our setup a 950 nm laser beam impinges first onto a set of 3.8 μm diameter silica microspheres located above the sample, producing a set of focal regions inside the sample matrix in which these ions are embedded. Because of the increase in the excitation per unit area in these focal regions, the upconverted emission, also coming from this area, attains a higher intensity value with respect to the bare substrate. Moreover, the microspheres can collect a certain solid angle of the total emission and redirect it in the backward direction resulting in an enhanced number of counts recorded by a properly positioned detector. From the detected image, the Full Width at Half Maximum (FWHM) of the emission in the focal area was obtained by deconvolution with the Point Spread Function (PSF) of the experimental system and compared with the theoretical value obtained with Finite-Differences Time-Domain (FDTD) simulations.

2. Experimental description

2.1. Preparation of the glass and glass ceramic samples

The samples were prepared using reagent-grade chemicals: (opti pure) SiO_2 (Alfa-aesar89709), Al_2O_3 (Alfa-aesar42571), CaF_2 (MERCK 102840 precipitated pure) ErF_3 (Alfa-aesar 13653) and YbF_3 (Across 31616) as raw materials. The batch compositions were mixed in agitate mortar for 10 min in a glove box with a humidity of less than 10%. The glass samples were prepared by melting the mixtures of the aforementioned materials in covered platinum crucibles at 1450 °C in an electric kiln for 90 min. The glasses were then annealed at 480 °C (close to the glass transition temperatures) for 3 h. The resulting samples were cut and polished to form 30 mm × 30 mm × 2 mm rectangular slices. The glass crystallization temperatures were determined by differential thermal analysis (DTA; Polymer Laboratories 1640, Amherst, MA). The ratio of SiO_2 to Al_2O_3 was chosen as 1.8 and 2.18 to fabricate two precursor glasses, fixing in both the dopant contents to 0.5 mol% of ErF_3 and 2 mol% of YbF_3 and the CaF_2 to 35 mol%. In what follows these glasses are referred to as SA1.8EY and SA2.18EY, respectively. In order to name the glass ceramic samples obtained from these precursor glasses, the thermal treatment temperature applied in each case was added to these names.

The glasses were heat treated in an electric kiln at three different temperatures (630, 675, and 690 °C) for 48 h, as per the DTA results, at a heating rate of 10 K/min. The crystalline phases, precipitated during the heat treatment, were identified with a Philips X'Pert Pro diffractometer equipped with a primary monochromator, Cu Kα radiation, and an X'Celerator detector. The presence of CaF_2 nanocrystals was confirmed with XRD patterns collected with a step of 0.016° in the 2θ angular range from 10° to 90° and an acquisition time of 2 h. The Debye–Scherrer formula yielded an average size of 25 nm for these nanocrystals.

2.2. Optical measurements with microspheres

The surface of each polished sample was covered with drops of a distilled water and silica microsphere solution (3.8 μm CoSpheric, Santa Barbara) and dried at room temperature so as to randomly spread the microspheres on the glass surface. The experimental setup in which the samples were imaged is shown in Fig. 1. The excitation beam from a 950 nm diode laser (L3-MSF03 JDS Uniphase) is directed by a beamsplitter to a microscope objective (Olympus Plan, 80x, NA = 0.9) used to produce a converging beam to illuminate the sample. After that, each microsphere focuses the 950 nm illumination near the surface of the sample, producing upconversion processes in the focal region. The excited Er^{3+}–Yb^{3+} ions emit at wavelengths centered on 545 nm and 650 nm, which can be easily detected. The emitted light goes through the microsphere and re-enters the microscope objective, being focused by a lens in a CCD camera (ATK-16HR). In order to select the red emission a proper combination of filters is placed before the CCD detector. The imaging system is characterized by its PSF with a value for the FWHM of 369 nm, which was obtained by the theoretical formula in Ref. [15] for this experimental setup.

3. Results and discussion

The emission spectra of the Er^{3+}–Yb^{3+} codoped SA1.8EY and SA2.18EY glasses and glass ceramics treated at 675 °C obtained under excitation at 950 nm are shown in Fig. 2a. The spectra were obtained from the bulk samples before covering them with microspheres. The main emission bands are in the green (at

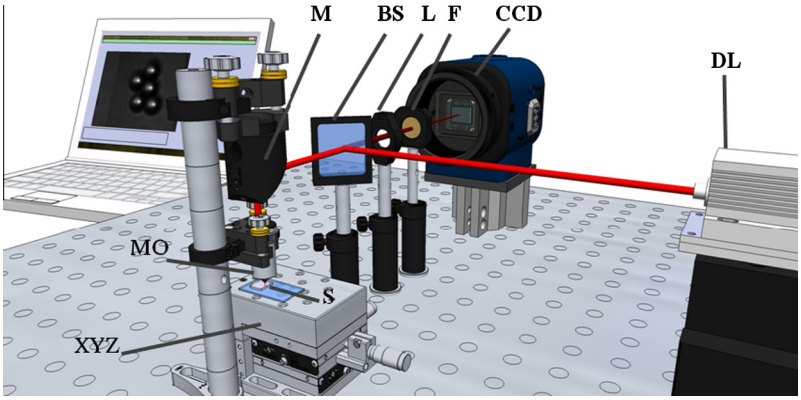

Fig. 1. Experimental setup. S. sample, XYZ. Three axis translation stage, M. Mirror, MO. Microscope objective, BS. Beamsplitter, L. Lens , F. Filter and DL. Diode Laser.

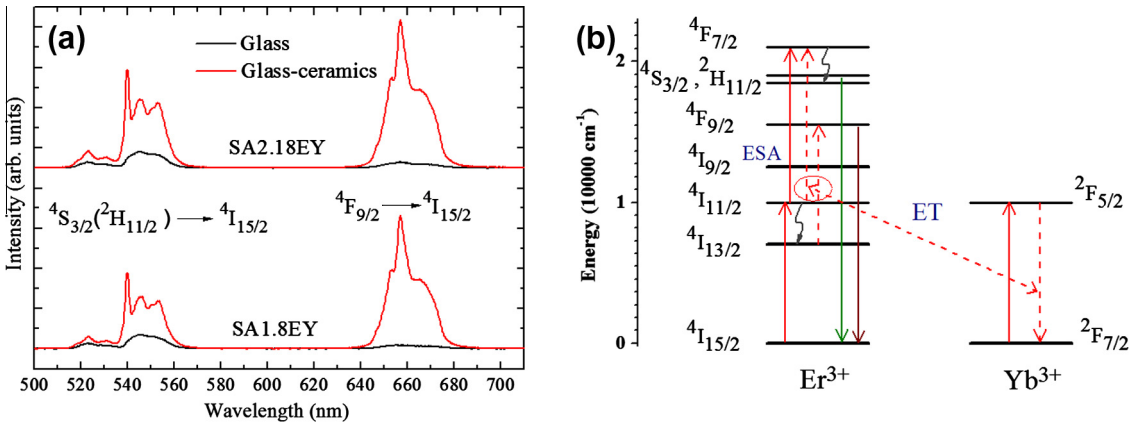

Fig. 2. (a) Upconversion emission spectra under excitation at 950 nm of Er^{3+}–Yb^{3+} doped glass and glass–ceramics obtained after a 675 °C thermal treatment in the SA1.8EY and SA2.18EY matrix. (b) Energy level diagrams of Er^{3+} and Yb^{3+} ions detailing ESA and ET upconversion processes.

545 nm, $^4S_{3/2}(^2H_{11/2}) \rightarrow {}^4I_{15/2}$) and red (at 650 nm, $^4F_{9/2} \rightarrow {}^4I_{15/2}$) regions. An explanation of how these transitions can take place is given in the diagram of Fig. 2b. The $^4F_{7/2}$ level can be populated after two possible upconversion processes called Excited State Absorption (ESA) and Energy Transfer (ET). In the ESA process, the Er^{3+} ion promotes from its ground state $^4I_{15/2}$ to the excited state $^4I_{11/2}$ and thereby to the $^4F_{7/2}$ by the direct absorption of two photons corresponding to the 950 nm excitation wavelength (indicated in the diagram by two solid red arrows). The energy overlap between the $^2F_{5/2}$ (Yb^{3+}) and the $^4I_{11/2}$ (Er^{3+}) levels enables the ET interaction (depicted in the diagram as dashed red arrows). In this process the Yb^{3+} ions reach the $^2F_{5/2}$ by the 950 nm excitation and in its de-excitation to the ground state $^2F_{7/2}$ transfers energy to an Er^{3+} ion in the $^4I_{11/2}$ level which reaches the $^4F_{7/2}$ level. The thermalized $^2H_{11/2}$ and $^4S_{3/2}$ levels are populated from the non-radiative de-excitation of the $^4F_{7/2}$ level. The green emission takes place after the relaxation of the $^4S_{3/2}$ to the ground state. As for the 650 nm emission band, it corresponds to the transition from the $^4F_{9/2}$ level to the ground state. This excited level can be populated from the upper thermalized levels ($^2H_{11/2}$ and $^4S_{3/2}$) or from ET processes from the $^4I_{13/2}$ levels, as indicated in Fig. 2b. These are likely mechanisms that are in agreement with the work in Ref. [16], indicating that both bands are generated by a two photon assisted process.

The emission spectra of the glass and glass ceramic samples treated at 675 °C are shown in Fig. 2a. The structured peaks in the glass ceramic samples are a characteristic feature of emissions from Er^{3+} ions immersed in crystalline environments. Especially noticeable is the higher intensity of the two emission bands in both glass ceramic samples over the glassy phase. The glass ceramic samples appear to confer an environment that benefits the upconversion processes in Er^{3+}–Yb^{3+} ions. This statement will be extensively explained later. To obtain the results shown below different filters were used in order to select the most intense radiation, which corresponds to the 650 nm red emission.

Fig. 3a shows an image of a six microsphere arrangement above the surface of an Er^{3+}–Yb^{3+} codoped SA1.8EY glass emitting at 650 nm. In Fig. 3b, a 3-D representation of the intensity distribution of this red emission is given. As can be seen in Fig. 3a, six independent narrow peaks emerge surrounded by a shadowed region. These more intense areas are enclosed within the contour of the circumferences, a clear indication that they are the result of the microlensing effect due to each sphere. This emission intensity comes from the 650 nm band produced by upconversion. The intensity gain, defined as the ratio of the maximum intensity and the mean value of the emission from the substrate, has a value of about 3, indicative of the enhanced upconversion process.

The dependence of the intensity at 650 nm with the pump power at the focal spot due to the microspheres and on the bare emitter substrate was also studied. It is widely known that the dependence of the upconversion emission intensity I_{UP} with the nth power of the IR excitation intensity I_{IR} follows the expression:

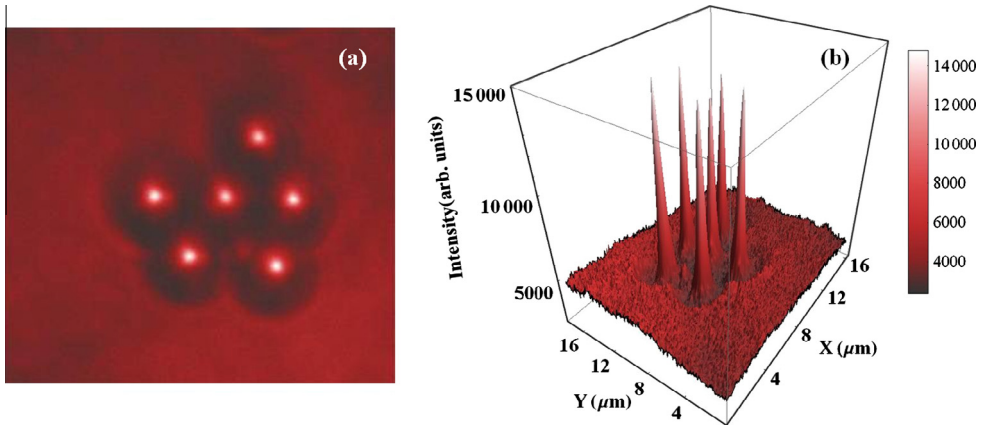

Fig. 3. (a) Image of the 650 nm emission of six microspheres located above an Er^{3+}–Yb^{3+} codoped SA1.8EY glass. (b) Right: 3D graph of the spatial intensity distribution of the red upconversion intensity corresponding to the left image. (For interpretation of the references to color in this figure legend, the reader is referred to the web version of this article.)

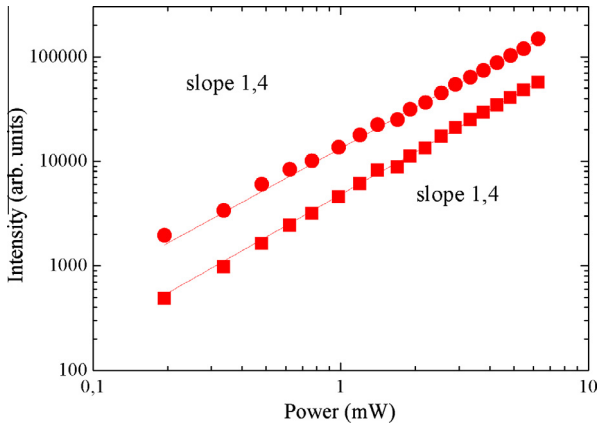

Fig. 4. Emission intensity for the 650 nm band obtained as a function of the 950 nm incident pump power collected from the flat glass sample (square) and through the microsphere (circles).

$$I_{UP} = AI_{IR}^{n} \quad (1)$$

where A is a constant and n is the number of IR photons absorbed per visible photon emitted. To perform the measurements, different pumping powers of the 950 nm laser were selected to take several images. The intensities collected inside the microsphere were, as expected based on Fig. 3a above the values obtained from the bare surface emission, with a factor 3 of mean gain. These results are plotted in a double-log scale in Fig. 4, where a linear dependence is observed. The two data sets have similar slopes with a value of around 1.4 for both the data collected inside and outside the microsphere. The reduction in the experimental value – with respect to the theoretical value of 2 – for an upconversion process that requires two photons, can be explained by the efficient upconversion rates in the levels involved [17]. Moreover, this nearly quadratic dependence is in good agreement with the upconversion mechanism explained before for the emission at 650 nm and obtained in other bulk samples without microspheres [16,18].

The results of the intensity counts reached at the microsphere focus for each sample and obtained under 950 nm with a pump power of 6.3 mW are given in Fig. 5. The two groups of samples, SA1.8EY and SA2.18EY, are plotted using different symbols for comparison. The X-axis shows the thermal temperatures at which the samples were heated to obtain nanocrystals, with the "glass" label on this axis corresponding to the precursor glass sample. As regards the addition of microspheres to these samples, in general, the upconversion luminescence tends to increase with rising heat treatment temperature, which leads to the incorporation of Er^{3+} ions into CaF_2 crystalline phase. Consequently, the upconversion intensity is increased significantly due to the decreased multiphonon relaxation at the higher heat treatment temperatures. This result is confirmed with the increase of the lifetimes of the levels involved in the upconversion processes. As an example, the lifetime of the $^4I_{11/2}$ level (see Fig. 2b) is increased from the 6.0 μs value obtained in the SA1.8EY glass sample to the 6.8 μs value when it is treated at 675 °C. Similarly, for the SA2.18EY glass sample a value of 5.9 μs is obtained, which increases to 6.8 μs when this sample is heat treated at 675 °C. This is why the upconversion emission obtained from the glass ceramic sample is much higher than in the precursor glass. Since Er^{3+} ions act as nucleate agents for CaF_2 crystals [19] during the heat treatment, Er^{3+} ions are incorporated in the CaF_2 crystals at the beginning of the formation of the CaF_2 crystals. The crystal size grew, increasing the heat treatment temperature, resulting in more Yb^{3+} ions near the surface of the crystals. According to the phase diagram of the CaF_2–YbF_3 system [20], CaF_2 and YbF_3 yield a solid solution in the range of about 0–35 mol% YbF_3 content. Therefore, the Yb^{3+} ions are considered to be incorporated into the CaF_2 to form $(Ca_{1-x}\,Yb_x)\,F_{2+x}$ solid-solution crystals during the heat treatment of the samples. According to the results shown in Fig. 5, increasing the heat treatment temperature led to a rise in the red emission of the upconversion luminescence of the SA2.18EY samples, whereas in the SA1.8EY samples there is an increase in the relative red emission until 675 °C followed by a decrease as the heat treatment temperature reaches 690 °C. In the glass with lower alumina content (SA2.18EY) and high viscosity, it seems that the majority of Yb^{3+} ions remain in the glass phase. In SA1.8EY at 690 °C there is a decrease in the red emission that could be explained by concentration quenching. As mentioned earlier, the Er^{3+} concentration in the CaF_2 nanocrystals in this sample is high. Moreover, high concentrations of Yb^{3+} ions were expected in this ratio due to the larger crystal size and the low viscosity of the glass. As a result, transfer and back transfer among these ions could be very efficient until the energy is transferred to traps. Based on this transfer, a decrease in the lifetime is predictable for the SA1.8EY samples at this temperature and a consequent reduction in the upconversion emission.

Another objective of this work is to analyze the size of the emission area (referred to in the following as upconversion spot) produced by each microsphere nanojet. So as to fully characterize the experimental upconversion spots, a representative profile for

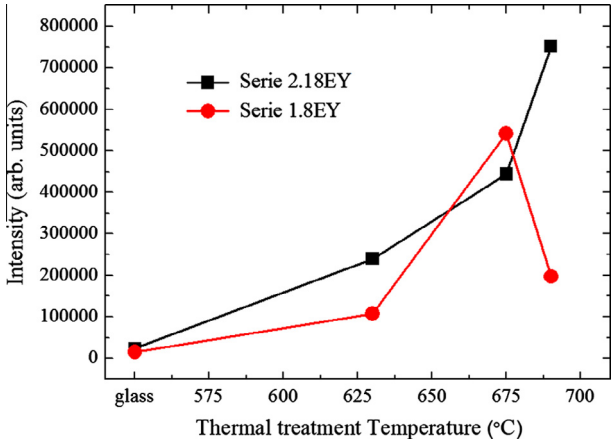

Fig. 5. Emission intensity collected through a microsphere as a function of the thermal treatment temperature applied to the following SiO_2/Al_2O_3 ratios: 1.8 (circles) and 2.18 (squares).

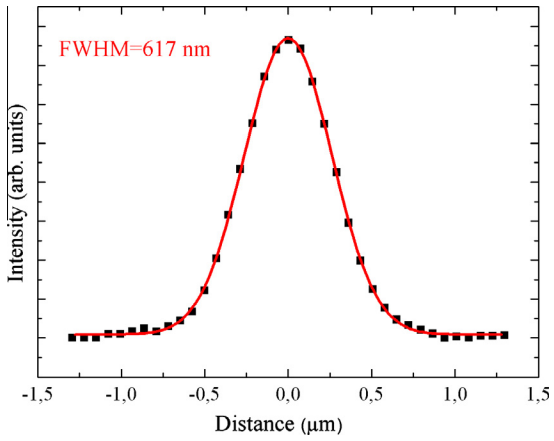

Fig. 6. Experimental intensity profile at a line that crosses the center of a microsphere (dots) and the Gaussian fit (continuous line).

one peak (from Fig. 3b) and the fit to a Gaussian profile are given in Fig. 6. As the figure reveals, the experimental data approach a Gaussian function, meaning its Full Width at Half Maximum (617 nm) can be considered a good estimate of the upconversion spot size. The real spot, however, is broadened by two factors. First, the PSF of the system, which cannot be directly subtracted from the measurement. In addition, the light emitted by the sample passes through the microsphere, which also increases or magnifies the spot size on its way to the detector. These two factors are taken into account in the following expression, obtained from the deconvolution properties of Gaussian functions [21], to yield the FWHM of the real spot:

$$W_{EXP}^2 = (W_{UPC}^{*}\beta)^2 + W_{PSF}^2 \quad (2)$$

where W_{EXP}, W_{UPC} and W_{PSF} represent the FWHM of the experimental measurement, the upconversion spot and the system PSF, respectively. The microsphere magnification β has a value of 1.5 and was measured by covering a diffraction grating (1200 lines/mm) with the microspheres under study and observing the grating lines through the sphere. As mentioned in the experimental description, the FWHM is 369 nm. Solving Eq. (2) returns a value of 330 nm for the FWHM of the upconversion spot.

The FWHM of the focal spot was also obtained by FDTD simulations, in a similar way to the calculations reported in Refs. [13,14,22]. The intensity distribution around a 3.8 μm silica microsphere illuminated by a 950 nm plane wave is shown in Fig. 7a. In order to compare with the experimental results, we must account for the fact that an upconversion process that requires two photon absorptions, like the one reported at 650 nm, is proportional to the square of the excitation power (see Eq. (1)). The transversal distributions at the focus maximum of the FDTD simulations are plotted in Fig. 7b, along with its square, which represents the emission spot. The calculation reveals a reduction from 453 nm, corresponding to the FWHM of a one photon density power, to a value of 320 nm for the red upconversion process. Taking into account the experimentally obtained value for the FWHM of 330 nm, we may conclude that this result is in good agreement with the theoretical calculations.

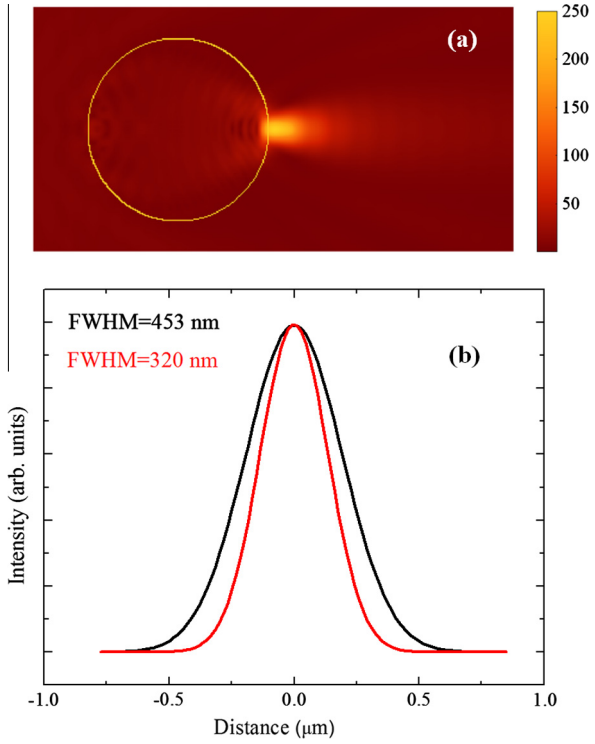

Fig. 7. (a) Intensity distribution at 950 nm obtained by FDTD simulation impinging from the left part of the image to a 3.8 μm diameter microsphere. (b) Transversal intensity profile at best focus for a one photon density power (black line) and two photon density power (red line). (For interpretation of the references to color in this figure legend, the reader is referred to the web version of this article.)

4. Conclusions

Upconversion processes in two sets of Er^{3+}–Yb^{3+} codoped glass and glass ceramics samples obtained with different thermal treatments have been analyzed under excitation at 950 nm. These processes were studied in bare bulk samples and also with the sample covered with 3.8 μm diameter silica microspheres. Since the microspheres act as microlenses of the IR excitation, the red intensity recorded around their focalized region is amplified with respect to the intensity emitted by the bare regions of the glass. This effect was studied in all the samples, with the resulting gain factor determined to be about 3. Measurements of the variation in the intensity emitted by the sample in the microsphere focus area and outside the microsphere with the pump power allowed us to conclude that the microspheres do not affect the upconversion mechanism. It was noted that the upconversion emission increases with thermal treatment temperature (630, 675 and 690 °C) in the glass ceramics with the highest Si/Al ratio (2.18). For the samples with a Si/Al ratio of 1.8, a gain in the upconversion emission was also observed, although the maximum value was obtained for 675 °C, meaning that the optimal thermal treatment has to be chosen properly.

The size of the emitting area was experimentally determined and yielded a FWHM of 330 nm, in close agreement with the Finite-Difference Time-Domain simulations (320 nm). This size could be reduced by using upconversion processes requiring more participating photons (three or four) and exciting at shorter wavelengths. These results could be applied to the detection of upconversion emission from small emitters.

Acknowledgements

Authors thank Ministerio de Economía y Competitividad of Spain (MINECO) within The National Program of Materials (MAT2010-21270-C04-02/-03/-04) and the Fundamental Research Program (FIS2012-38244-C02-01), The Consolider-Ingenio 2010 Program (MALTA CSD2007-0045, www.malta-consolider.com), the EU-FEDER for their Financial Support, the FSE and ACIISI of Gobierno de Canarias for the Project ID20100152 and FPI grant. We also thank The Governments of Spain and India for the award of a project within the Indo–Spanish Joint Programme of Cooperation in Science and Technology (PRI–PIBIN-2011-1153/DST-INT-Spain-P-38-11).

References

[1] D. Jaque, F. Vetrone, Nanoscale 4 (2012) 4301.
[2] K.A. Willets, S.Y. Nishimura, P.J. Schuck, R.J. Twieg, W.E. Moerner, Acc. Chem. Res. 38 (2005) 549.
[3] C.M. Luk, L.B. Tang, W.F. Zhang, S.F. Yu, K.S. Teng, S.P. Lau, J. Mater. Chem. 22 (2012) 22378.
[4] J. Boyer, L.A. Cuccia, J.A. Capobianco, Nano Lett. (2007) 847.
[5] F.D. Stefani, J.P. Hoogenboom, E. Barkai, Phys. Today (2009) 34.
[6] D.H. Kim, J.U. Kang, Microscopy: Science, Technology, Applications and Education, in: A. Méndez-Vilas, J. Díaz (Eds.), FORMATEX Microscopy Series n° 4, Vol. 3, (2010) 571–582.
[7] L.L. Martín, I.R. Martín, P. Haro-González, J. Lumin. 131 (2011) 2446.
[8] F. Lahoz, N. Capuj, P. Haro-González, I.R. Martín, C. Pérez-Rodríguez, J.M. Cáceres, J. Appl. Phys. 109 (2011) 043102.
[9] V.B. Alexander Heifetz, Soon-Cheol Kong, Alan V Sahakian, Allen Taflove, J. Comput. Theorical Nanosci. 6 (2009) 1979.

[10] K.W. Allen, A. Darafsheh, V.N. Astratov 13th Int. Conf. Transparent Opt. Networks (2011) 1.
[11] A. Heifetz, K. Huang, A.V. Sahakian, X. Li, A. Taflove, V. Backman, Appl. Phys. Lett. 89 (2006) 221118.
[12] S. Yang, A. Taflove, Opt. Express 19 (2011) 7084.
[13] S.C. Hill, V. Boutou, J. Yu, S. Ramstein, J. Wolf, Y. Pan, S. Holler, R.K. Chang, Phys. Rev. Lett. 85 (2000) 54.
[14] S. Lecler, S. Haacke, N. Lecong, O. Crégut, J.-L. Rehspringer, C. Hirlimann, Opt. Express 15 (2007) 4935.
[15] R.W. Cole, T. Jinadasa, C.M. Brown, Nat. Protoc. 6 (2011) 1929.
[16] Z.X. Cheng, S.J. Zhang, F. Song, H.C. Guo, J.R. Han, H.C. Chen, J. Phys. Chem. Solids 63 (2011) 2011.
[17] M. Pollnau, D. Gamelin, S. Lüthi, Phys. Rev. B 61 (2000).
[18] I.R. Martín, P. Vélez, V.D. Rodríguez, U.R. Rodríguez-Mendoza, V. Lavín, Spectrochim. Acta A 55 (1999) 935.
[19] D. Chen, Y. Wang, Y. Yu, E. Ma, F. Bao, Z. Hu, Y. Cheng, Mater. Chem. Phys. 95 (2006) 264.
[20] D. Chen, Y. Wang, E. Ma, Y. Yu, F. Liu, Opt. Mater. 29 (2007) 1693.
[21] P. Ferrand, J. Wenger, A. Devilez, M. Pianta, Opt. Express 16 (2008) 209.
[22] S.-C. Kong, A. Sahakian, A. Taflove, V. Backman, Opt. Express 16 (2008) 13713.